Korean J. Chem. Eng., **20**(5), 950-955 (2003)

Utilization of Mesoporous Molecular Sieves Synthesized from Natural Source Rice Husk Silica to Chlorinated Volatile Organic Compounds (CVOCs) Adsorption

Nurak Grisdanurak†, Siriluk Chiarakorn* and Jatuporn Wittayakun**

Catalytic and Material Research Laboratory, Department of Chemical Engineering, Khon Kaen University, Khon Kaen, 40002, Thailand
*National Research Center for Environmental and Hazardous Waste Management,
Chulalongkorn University, Bangkok, 10330, Thailand
**School of Chemistry, Suranaree University of Technology, Nakhon Ratchasima, 30000, Thailand
(Received 18 November 2002 • accepted 13 May 2003)

Abstract—The adsorption of trichloroethylene (TCE), tetrachloroethylene (PCE), and carbon tetrachloride was studied over our synthesized mesoporous material, MCM-41, from rice husk silica source, abbreviated as RH-MCM-41. More than 99% silica for RH-MCM-41 synthesis was extracted from rice husk under refluxing in HBr solution and then calcined at 873 K for 4 hours. RH-MCM-41 possessed surface area around 750-1,100 m^2/g with a uniform pore size with an average diameter of 2.95 nm, narrow range of pore distribution and somewhat hexagonal structure, similar to properties of parent MCM-41. The adsorption of CCl_4 to RH-MCM-41 was stronger than that of TCE and PCE. The adsorption capacity of RH-MCM-41 for CVOCs (chlorinated volatile organic compounds) was higher than commercial mordenite and activated carbons.

Key words: MCM-41, Chlorinated Volatile Organic Compounds (CVOCs), Adsorption, Rice Husk Silica

INTRODUCTION

Volatile organic compounds (VOCs), which are widely used in industrial solvents, cleaners, etc., are major air pollutants that must be controlled under the increasingly stringent environmental regulations. Chlorinated volatile organic compounds (CVOCs) possess more severe properties than other VOCs categories. CVOCs found in industrial chemicals can produce hazardous and toxic wastes. In addition, high temperature possibly increases free chlorine radical in the atmosphere, which can destroy the ozone layer [Faisal et al., 2000]. The simplest subgroup of the chlorinated hydrocarbon family is composed of chlorinated methanes including methyl chloride (CH_3Cl), methylene chloride (CH_2Cl_2), chloroform ($CHCl_3$), and carbon tetrachloride (CCl_4). They are used for dry cleaning of fabrics, metal-degreasing, and as starting material for other chemicals and consumer products. The difficulty in incinerating treatment of these compounds is ranked from the higher Cl^- content. Further treatment, like adsorption, is needed and can overcome the difficulties from conventional incineration of the gaseous effluent containing CVOCs. Recent adsorption/separation technology employing activated carbon adsorbents is commonly used in industry because of the easy operation and low operating cost. However, it has a few problems such as combustion of adsorbents and pore blocking [Zhao et al., 1998, 2001]. Therefore, several researchers have focused on finding alternative adsorbents. Hydrophobic zeolite adsorbents have been proven to be an advancement in VOCs adsorption/separation technology because they could overcome the problems associated with activated carbon adsorbents [Anderson, 2000; Choudhary, 1996].

Since the past decade, M41S has been studied widely. It is generally synthesized by an addition of aqueous solution containing silica (e.g., fume silica, sodium silicate) to a clear aqueous solution of a micelle-forming surfactant (e.g., long-chain quaternary ammonium halides) under hydrothermal conditions [Selvam et al., 2001; Zhao et al., 1998; Kim et al., 2000]. A number of parameters during the preparation which can affect the resultant phases include pH, mole ratio of reactants, aging, stirring, adding sequence of reactants, etc. [Huo et al., 1994]. The resulting material shows a hexagonal array of uniform mesoporous, which depends on the type of template and synthesis conditions and has narrow pore size distribution tunable from 2.0 to 10 nm, large surface area and one-dimensional pores [Ole et al., 2001; Selvam et al., 2001; Zhao et al., 1998]. Because of its distinguishable properties, potential applications of MCM-41 are as exciting as its discovery and a number of applications have been investigated. One attractive application is to use MCM-41 as an adsorbent for VOC control [Namba et al., 1997; Jänchen et al., 1997].

Because siliceous material is needed for zeolite synthesis, rice husk can serve as an alternative silica source. It is one type of biomass available globally with approximately 100 million tons being generated annually worldwide. Although rice husk has basic usage as burning fuel for electricity generation, its ash disposal as waste is an environmental issue due to its particulate dispersion. In Thailand, a large amount of rice husk is produced and practically used later in agricultural field and/or power plant as low-value material. From our previous study, high purity silica could be produced from rice husk and could be utilized more efficiently as a silica source for zeolite synthesis. In this study rice husk is used as a silica source to produce MCM-41 which will be referred to as RH-MCM-41 throughout this article. Details given here include RH-MCM-41 synthesis, its utilization as an adsorbent for CVOCs, and regeneration of RH-MCM-41 after adsorption. Furthermore, the energy of desorption was determined by CVOCs temperature-programmed desorption (TPD) in a thermogravimetric analyzer (TGA).

†To whom correspondence should be addressed.
E-mail: nurgri@mail.kku.ac.th

EXPERIMENTAL

1. Preparation of the RH-MCM-41

Silica was extracted from rice husk (RH) under refluxing in HBr solution, washed with water, and then calcined at 873 K for 4 hours. Afterwards, it was dissolved with sodium hydroxide to form sodium silicate.

RH-MCM-41 was prepared by using hexadecyltriammonium bromide (CTABr) as a template and sodium silicate from rice husk. The molar ratios of reactant were 0.147 CTABr : 1 SiO_2 : 2.16 NH_4OH : 148.94 H_2O. CTABr was dissolved in deionized water until a clear solution was obtained before an addition of ammonium hydroxide and tetraorthosilicate to form precipitation. Finally, the suspended solid was filtered, washed, and dried at 373 K for 1 hour. The product after drying was calcined in air flow at 873 K for 6 hours. In addition, parent MCM-41 was synthesized as a reference material by procedures described by Beck et al. [1992].

2. Characterization of RH-MCM-41

2-1. X-Ray Diffraction (XRD)

Powder XRD patterns were obtained from a Bruker axs D5005 diffractometer. The x-ray was generated from a Cu Kα target with a current of 40 mA and a potential of 40 kV. The scan was performed between 2θ values of 1 and 10 degrees at a scan rate of 0.06 degrees per minute.

2-2. N_2 Adsorption Isotherms and BET Surface Area

The isotherm and surface area was obtained by the most common adsorbate, N_2, at 77 K on a Micromeritics ASAP 2010 sorption analyzer where nitrogen adsorption and desorption isotherms were measured. Before measurement, samples were pretreated with heat at 378 K overnight to remove moisture. Specific surface areas of the studied materials were calculated by using the standard BET method at the relative pressure range of 0.05-0.30. Pore diameters were estimated from the peak positions of BJH pore size distribution curves calculated from the adsorption isotherms. The mesoporous volumes were estimated from the amount adsorbed at the relative pressure of about 0.95.

2-3. Scanning Electron Microscope (SEM)

Powder sample was sprinkled in a thin layer on an adhesive tape on a brass bar. Excess amount was blown away by air spray. The sample was then coated with gold by JEOL (JFC-1100E Ion) sputtering device and transferred into the JEOL (JSM-6400) sample chamber where an accelerating voltage of 15-40 kV was used.

2-4. Transmission Electron Microscope (TEM)

Prepared specimens were deposited on a grid copper grid 300 mesh and rapidly transferred to a JEOL-JEM-200 CX transmission electron microscope operated at 100 kV.

2-5. Fourier Transform Infrared Spectrometry (FTIR)

The sample was ground by an agate mortar and pestle until it had approximately the same consistency as the KBr powder. KBr was added, mixed thoroughly, and the mixture powder was poured into the sample barrel and pressed at 13 tons for 1 minute before being put on a V-mount cell. The FTIR spectrum was recorded in the 400-4,000 cm^{-1} range.

2-6. Adsorption Behavior Study

A certain amount of RH-MCM-41 was loaded into each studied CVOC solution and kept for equilibrium time. RH-MCM-41 was filtered and dried over 383 K for 4 hours before the known amount was placed on a platinum pan and later placed inside a TGA analysis. The weight loss due to desorption during temperature programmed with the heating rate of 5 K min^{-1} was recorded.

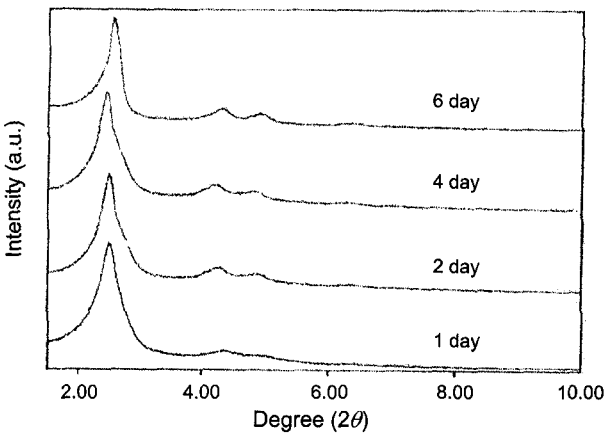

Fig. 1. X-ray powder diffraction patterns of RH-MCM-41 from different aging time: (a) 24 h, (b) 48 h, (c) 96 h, and (d) 144 h.

RESULTS AND DISCUSSION

1. XRD

The mesoporous materials, RH-MCM-41, which originated from the same initial gels, collected at a reaction times of 24, 48, 96, and 144 hours under typical synthetic conditions, gave the XRD patterns shown in Fig. 1. The 2θ values at 2.4, 4.0, 4.4, and 6 degrees corresponding to the *hkl* reflection plane 100, 110, 200, and 210, respectively, were in good agreement with the pattern from a pure siliceous MCM-41 reported elsewhere [Legrand, 1998]. XRD spectrum indicated that 48 hours was a sufficient synthesis time. Moreover, the average crystallite diameters (t) were calculated from Scherrer formula [Eq. (1)]:

$$t = \frac{0.9\lambda}{\beta\cos\theta_B} \quad (1)$$

where λ is the X-ray wavelength, $\beta=(B-b)^{1/2}$, B is the breadth at half the maximum intensity of the sample, b is the breadth at half the maximum intensity of standard, and θ_B is diffraction angle. The average crystallite diameters at the different aging time are shown in Table 1. The mean crystallite diameter at various aging times indicated that the particle size inversely depends on aging time.

2. N_2 Adsorption Isotherms and BET Surface Area

The N_2 adsorption isotherm for the calcined RH-MCM-41 is shown in Fig. 2. A sharp increase between relative pressure P/Po

Table 1. Mean crystalline diameters of RH-MCM-41 with various aging times

Aging time (h)	B	b	Mean crystallite diameter (nm)
24	0.24	0.2	1.05
48	0.26	0.2	0.84
96	0.29	0.2	0.66
144	0.30	0.2	0.64

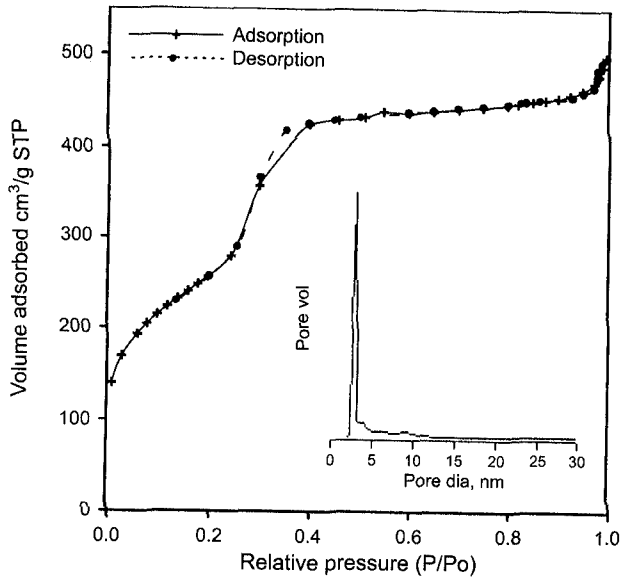

Fig. 2. Adsorption (solid line) and desorption (dotted line) isotherms of N_2 at 77 K on RH-MCM-41 from aging time of 48 h.

of 0.25 and 0.35 corresponds to capillary condensation within uniform mesopores. No significant hysteresis loop in the adsorption and desorption cycle upon pore condensation was observed, which indicated that RH-MCM-41 has large pore size. The adsorption of N_2 isotherm over RH-MCM-41 was type IV, which was a character of highly porous and one dimensional material. The very narrow PSDs (pore size distributions) and no observation of microporous are shown inside Fig. 2. Furthermore, the mesophase synthesized in this work contained only pure MCM-41 material without the presence of any microporous and/or amorphous phases. Comparison of RH-MCM-41 surface properties with references is shown in Table 2.

3. SEM and TEM

Fig. 3 shows surface morphology of RH-MCM-41 with 48 hours aging time from SEM analysis at the magnification of 20,000. However, SEM could not identify the structure clearly since the magnification was not high enough to see small details. Only white bulky cylindrical solid was observed indicating only the formation of hexagonal rods. The information of hexagonal array could be explained by TEM images as shown in Fig. 4.

4. FTIR

Infrared spectroscopy can be used for both qualitative and quantitative analysis of molecular species. The most widely used region is the mid-infrared that extends from about 400 to 4,000 cm^{-1} (wavelength 2.5 to 14.9 μm, respectively). FTIR spectra of RH-MCM-

Table 2. Comparison of RH-MCM-41 surface properties with those from some references

Sample	D_{pore} (nm)	V_{pore} (ml/g)	S_{BET} (m^2/g)
RH-MCM-41 (this work)	2.95	0.869	775-1,100
MCM-41[a]	2.95	0.91	1,180
MCM-41[b]	3.92	1.33	1,139
Actovated carbons	~6-20		~1,200

[a]3 day aging time at 373 K in a stainless steel autoclave [Zhao, 2000].
[b]6 day aging time at 373 K in a stainless stell autoclave [Yingcai, 1998].

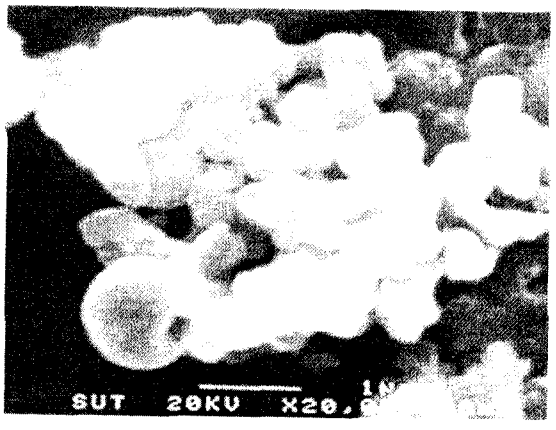

Fig. 3. SEM image of RH-MCM-41 from aging time of 48 h.

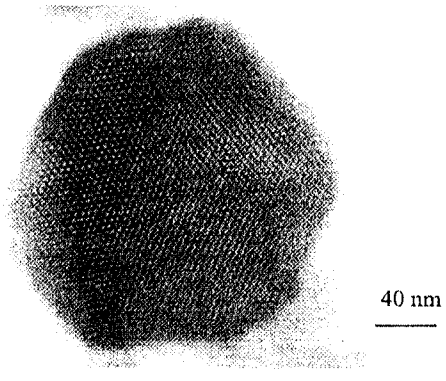

Fig. 4. TEM image of RH-MCM-41 from aging time of 48 h.

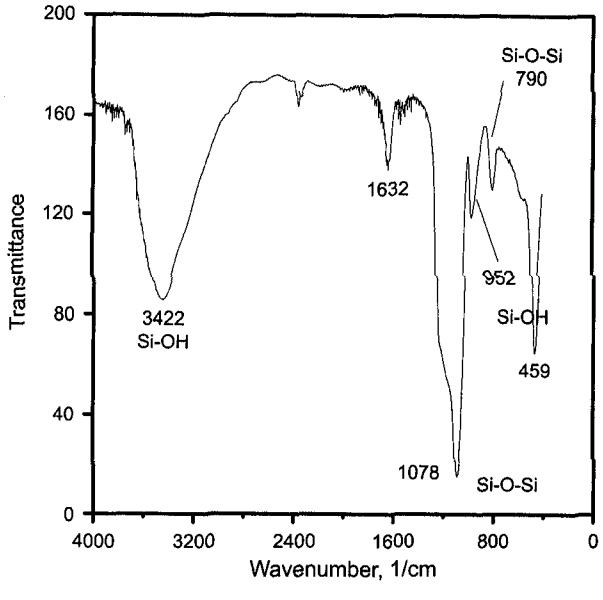

Fig. 5. FTIR spectra of RH-MCM-41 from aging time of 48 h.

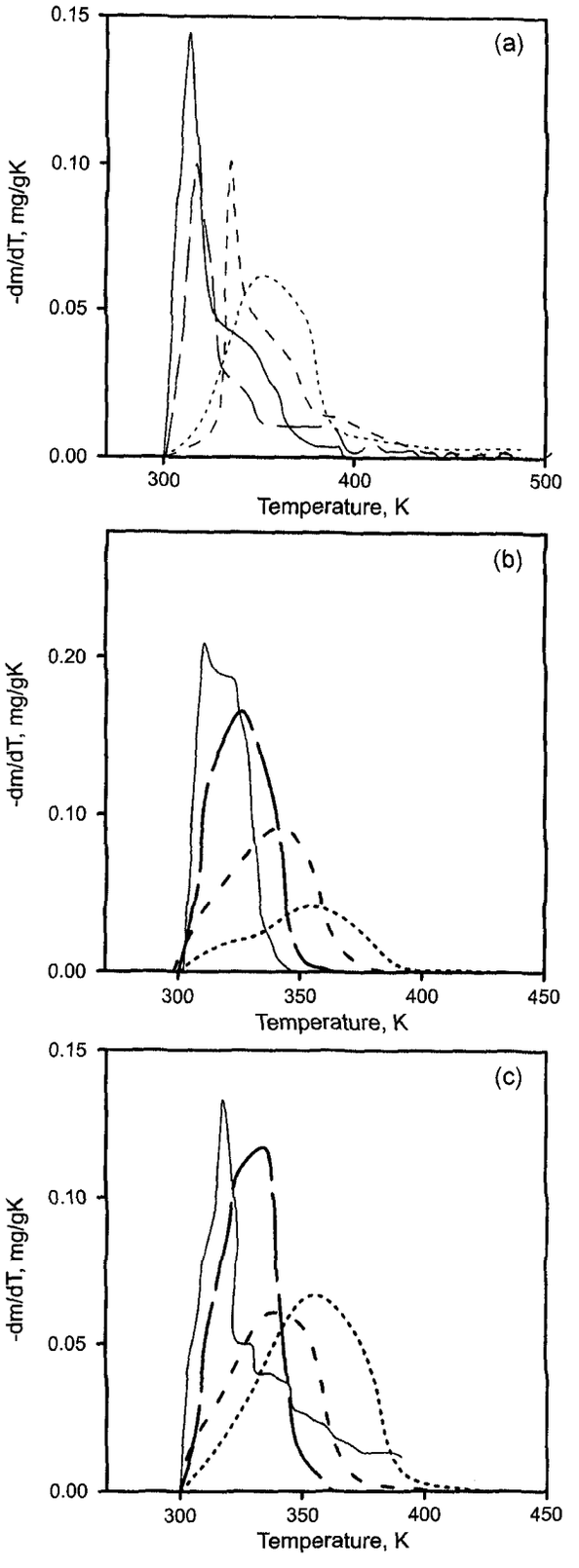

Fig. 6. TPD profiles of (a) TCE, (b) PCE and (c) CCl_4 from RH-MCM-41 at various heating rates.
—— 3 K min^{-1}, —— 5 K min^{-1}, ----- 12 K min^{-1}, ····· 20 K min^{-1}

41 in transmittance modes are shown in Fig. 5.

A broad absorption band around 3,400 cm^{-1} was assigned to H-bonded silanols brought close to other silanols (Si-O-H) acting as proton acceptors [Romero et al., 1997]. The sample also showed a peak at 790 cm^{-1} attributed to symmetrical Si-O-Si stretching vibration while the peak at 952 cm^{-1} was assigned to symmetric stretching vibration of Si-O-H groups [Zhao et al., 2000]. Since the measurement was taken at ambient condition, a weak peak at 2,354 cm^{-1} was caused by CO_2 vibration peak. A strong peak at 1,087 cm^{-1} was referred to Si-O-Si anti-symmetric stretching. These results confirm that the surface of RH-MCM-41 possess silanol groups, the required adsorption sites.

5. Adsorption

In our study, adsorption behavior was studied in terms of chemical desorption of TCE, PCE, and CCl_4 with increasing temperature rates of 3, 5, 12, and 20 K min^{-1}. Fig. 6 shows the inverse-derivative peak of desorption (-dm/dT) from temperature programmed desorption of each chemical with different increasing temperature rates. Weight loss by the dehydroxylation during the thermal desorption could be ignored. This was in accordance with the fact that samples of RH-MCM-41 were activated at 873 K for 6 hours before adsorption tests. Since there is no aluminum presence in the RH-MCM-41 samples, the catalytic effect brought about by acidic sites during the thermal desorption could be neglected. Area under the desorption peak represented the adsorbed amount. In this study, only positions of maximum temperatures for each weight loss spectrum were our concern.

The maximum peaks for TCE were shifted from 313 to 316, 334, and 355 K (Fig. 6a), according to the increasing heating rate. It revealed the chemical desorption from the surface before reaching its boiling point (360 K). Like the TPD spectrum of TCE, it was found similar to other TPD spectra of PCE and CCl_4. The maximum peaks for PCE were 310.8, 325.5, 343.3, and 352.6 (Fig. 6b). Those data

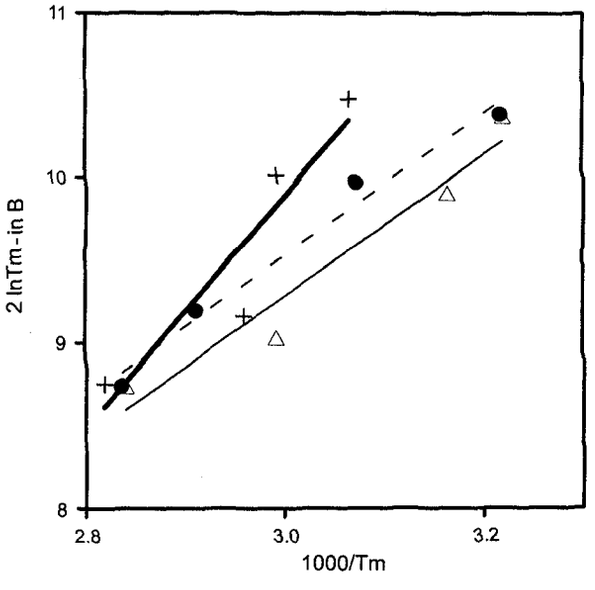

Fig. 7. Plot of $2\ln T_m$-lnB value as a function of $1000/T_m$ of RH-MCM-41 from aging time of 48 h.
—— TCE, ····· PCE, —— CCl_4

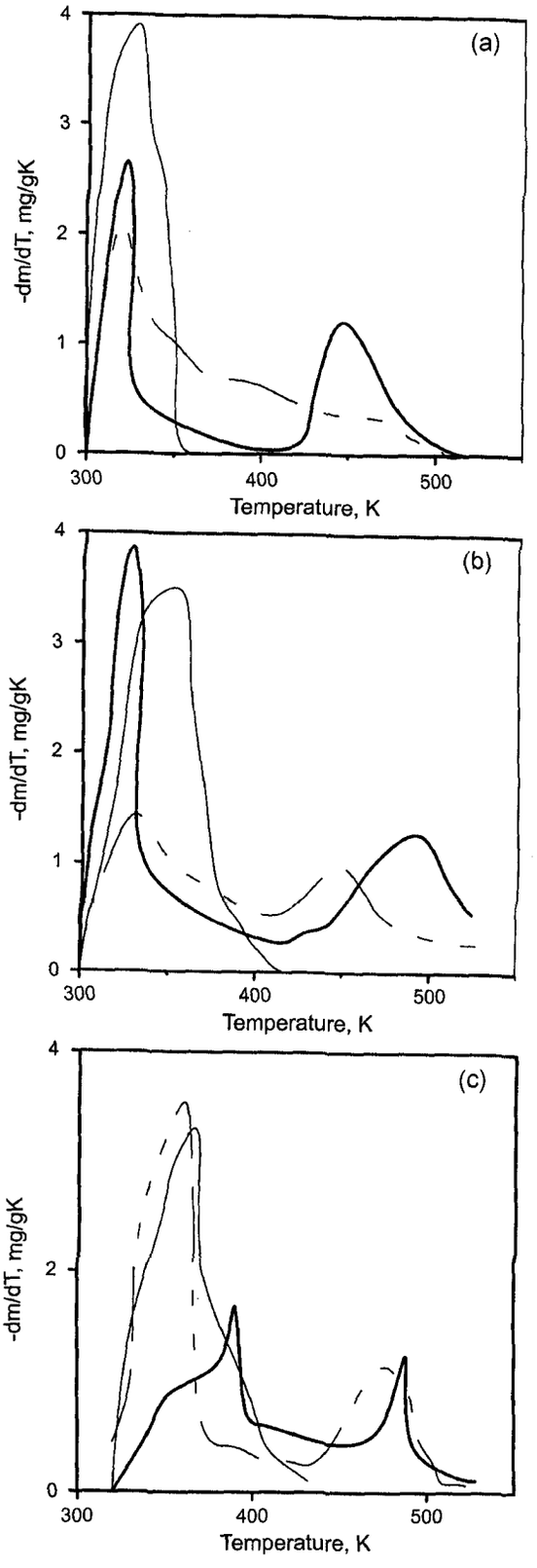

Fig. 8. TPD profiles of CVOCs at various heating rate 5 K min^{-1} *on various adsorbents.*
—— RH-MCM-41, ---- Mordenite, —— Activated carbons, (a) TCE, (b) PCE, (c) CCl_4

were lower than its boiling (393 K). The maximum peaks for CCl_4 were 326.2, 334.1, 337.8, and 354.8 K (Fig. 6c), which were partially close to its boiling point (350 K). It was found that, for all chemicals, maximum peaks moved to the higher temperatures corresponding to higher increasing temperature rate.

The maximum peaks of each heating rate were plotted in the form of natural log value versus reversed maximum peaks as the Eq. (2) [Zhao et al., 2001].

$$2\ln T_m - \ln B = \frac{E_d}{RT_m} + \frac{E_d}{AR} \quad (2)$$

The parameter T_m is maximum temperature weight loss (K), B is a heating rate, (K min^{-1}), E_d/AR is a constant. The plot from Eq. (2) would provide adsorption energy by its slope, shown in Fig. 7.

The slope for TCE, PCE, and CCl_4 were 4.29, 4.32, and 7.03, respectively, corresponding to the calculated adsorption energy of 35.6, 35.9, and 58.4 kJ/mol, respectively. The order of adsorption energy declined from CCl_4, PCE, to TCE. TCE and PCE somewhat adsorbed with moderate adsorption energy, while CCl_4 adsorbed more strongly, probably with covalent bond. After considering TPD of chemicals at a constant heating rate of 5 K min^{-1}, it showed the RH-MCM-41 provided the similar amount of chemical sorption uptake for all three chemicals

6. Regeneration Capacity and Comparison

In addition, we attempted to compare the adsorption results from this work with commercial adsorbents including mordenite (ratio of Si/Al=19, sodium form) and activated carbon. The capability for the adsorption of CVOCs of each sorbent was investigated and compared.

The properties of commercial adsorbents and RH-MCM-41 are shown in Table 1 and TPD profiles of CVOCs on varied adsorbents are shown in Fig. 8. Considering areas under the adsorption peaks, the best adsorption capacity for CVOCs was observed on RH-MCM-41. Moreover, RH-MCM-41 was the only material that adsorbed CVOCs by a single type of active site because RH-MCM-41 possessed a uniform pore size diameter, and large enough for CVOCs to adsorb uniformly [Zhao et al., 2000]. One peak at comparatively low temperature in the desorption profile on RH-MCM-41 suggested self-blocking of the channel network. This information would be useful for further catalytic application. It has been reported that TPD spectra of organic compounds from microporous zeolite frequently display two-stage desorption processes due to self-blocking of the channel network by flexible molecules bending through 90° at intersections of the channel system [Richards and Rees, 1986]. Obviously, activated carbon showed two desorption peaks for all tested CVOCs and mordenite showed two peaks for PCE and CCl_4 indicating that they have two different active sites or two different pore dimensions. Both mordenite and activated carbon have micropores and mesopores which could be responsible for those two desorption peaks. This result revealed that high temperature was required for the adsorbent regeneration which, however, might gradually damage surface structure.

CONCLUSION

RH-MCM-41 was synthesized by micelle form at 303 K and vigorous stir with aging time of 48 hours or more. It possessed a sur-

face area around 750-1,100 m^2 g^{-1} with an average pore diameter of about 2.95 nm. The pore distribution was narrow in the range of 20-35 nm. RH-MCM-41 adsorbed each of the three chemicals in similar amount, but the adsorbed CCl_4 was stronger than TCE and PCE. RH-MCM-41 had only one kind of active site for adsorption of CVOCs. In contrast, all studied CVOCs adsorbed over 2 active sites of activated carbon. TCE and PCE adsorbed over mordenite on a single site, while CCl_4 adsorbed one 2 active sites. The amount of adsorbed TCE on RH-MCM-41 was greater than that on activated carbon and mordenite. However, PCE and CCl_4 adsorbed on RH-MCM-41 as much as activated carbon but more than mordenite.

ACKNOWLEDGMENTS

This research was carried out under a contract by National Metal and Materials Technology Center, Thailand (MT-B-45-CER-12-136-G). The National Research Center of Environmental Hazardous Waste Management, Khon Kaen University Network, was also gratefully acknowledged.

REFERENCES

Anderson, M. A., "Removal of MTBE and Other Organic Contaminants from Water by Sorption to High Silica Zeolites," *Environ. Sci. Technol.*, **34**, 725 (2000).

Beck, J. S., Vartuli, C., Roth, W. J., Leonowicz, M. E., Kresge, C. T., Schmitt, K. D., Chu, T.-W., Olson, D. H., Sheppard, E. W., McCullen, S. B., Higgins, J. B. and Schelenker, J. L., "A New Family of Mesoporous Molecular Sieves Prepared with Liquid Crystal Templates," *J. Am. Chem. Soc.*, **114**, 10834 (1992).

Choudhary, V. R. and Mayadevi, S., "Adsorption of Methane Ethane and Ethylene and Carbon Dioxide on Silicalite," *Zeolites*, **17**, 501 (1996).

Faisal, I. K. and Aloke, K. G., "Review Removal of Volatile Organic Compounds from Air Pollution," *J. Loss Prevent. Proc.*, **13**, 527 (2000).

Huo, Q., Margolese, D. L., Ciesla, U., Feng, P., Gier, T. E., Sieger, P., Leon, R., Retroff, P. M., Schüth, F. and Stucky, G. D., "Generalized Synthesis of Periodic Surfactant Inorganic Composite Materials," *Nature*, **368**, 317 (1994).

Jächen, J., Busio, M., Hintze, M., Stach, H. and van Hooff, J. H. C., "Adsorption Studies on Ordered Mesoporous Materials (MCM-41)," *Stud. Surf. Sci. Catal.*, **105**, 1731 (1997).

Kim, G.-J., Park, D.-K. and Ha, J.-M., "Synthesis of a Siliceous MCM-41 Using C_{22}TMACl Template and Preparation of Heterogenized New Chiral Salen Complexs," *Korean J. Chem. Eng.*, **17**, 337 (2000).

Legrand, P. A., "The Surface Properties of Silicas," John Wiley & Sons, Inc., England (1998).

Namba, S., Sugiyama, N., Yamai, M., Shimamura, I., Akoki, S. and Izumi, J., "Pressure Swing Adsorption of Organic Solvent Vapors on Mesoporous Silica Molecular Sieves," *Stud. Surf. Sci. Catal.*, **105**, 17891 (1997).

Ole, G., Sjoblom, J. and Stocker, M., "Synthesis, Characterization and Potential Applications of New Materials in the Mesoporous Range," *Adv. Colliod Interfac.*, **89-90**, 439 (2001).

Richards, R. E. and Rees, L. V., "Temperature Programmed Desorption of Sorbates from Zeolites Part I. Constant Coverage, Variable Heating Rate Method," *Zeolites*, **6**, 17 (1986).

Romero, A. A., Alba, M. D., Shou, W. K. and Klinoski, J., "Synthesis and Characterization of the Mesoporous Silicate Molecular Sieve MCM-48," *J. Phys. Chem. B.*, **101**, 5294 (1997).

Selvam, P., Bhatia, K. S. and Sonwane, G. C., "Review Recent Advances in Processing and Characterization of Periodic Mesoporous MCM-41 Silicate Molecular Sieves," *Ind. Eng. Chem. Res.*, **40**, 3237 (2001).

Silverstein, R. M., "Spectrometric Identification of Organic Compounds," John Wiley & Sons, Inc., Singapore (1995).

Wang, H. P., Lin, K.-S., Huang, Y. J., Li, M. C. and Tsau, L. K., "Synthesis of Zeolite ZSM-48 from Rice Husk Ash," *J. Hazard. Mater.*, **58**, 147 (1998).

Yingcai, L., Taiming, X., Yaojun, S. and Weiyang, D., "Adsorption Behavior on Defect Structure of Mesoporous Molecular Sieves MCM-41," *Langmuir*, **14**, 6173 (1998).

Zhao, X. S., Ma, Q. and Lu, G. Q., "VOCs Removal: Comparison of MCM-41 with Hydrophobic Zeolite and Activated Carbon," *Energ Fuel*, **12**, 1051 (1998).

Zhao, X. S., Lu, G. Q. and Hu, X., "Characterization of the Structural and Surface Properties of Chemically Modified MCM-41 Materials," *Micropor Mesopor Mat.*, **41**, 37 (2000).

Zhao, X. S., Lu, G. Q. and Hu, X., "Organophilicity of MCM-41 Adsorbents Studied by Adsorption and Temperature-Programmed Desorption," *J. Therm. Anal. A: Physicochem. Eng. Aspcs.*, **179**, 261 (2001).